EXPOSING IMAGE FORGERY THROUGH THE DETECTION OF CONTRAST ENHANCEMENT

Xufeng Lin[1], Chang-Tsun Li[1] and Yongjian Hu[1,2]

[1]Department of Computer Science, University of Warwick, UK
[2]South China University of Technology, Guangzhou, China

ABSTRACT

In this paper, a novel forensic method of exposing cut-and-paste image forgery through detecting contrast enhancement is proposed. We reveal the inter-channel correlation introduced by color image interpolation, and show how a linear or nonlinear contrast enhancement can disturb this natural inter-channel dependency. We then construct a metric to measure these correlations, which are useful in distinguishing the original and contrast enhanced images. The effectiveness of the proposed algorithm is experimentally validated on natural color images captured by commercial cameras. Finally, its robustness against some anti-forensic algorithms is also discussed.

Index Terms— Digital forensics, contrast enhancement, demosaicking, inter-channel correlation

1. INTRODUCTION

In an image subjected to the typical cut-and-paste forgery, the contrast between the background and the pasted region is not usually consistent with that of the original image due to different lighting conditions. Consequently, contrast enhancement is widely used by the attacker to avoid leaving obvious visual clues after forging an image. However, a number of contrast enhancement operations are equivalent to pixel value mappings, which introduce some statistical traces. Therefore, we can expose cut-and-paste image forgery by detecting contrast enhancement. A blind method is proposed in [1] to detect globally and locally applied contrast enhancement operations, which introduce sudden peaks and zeros in the histogram and therefore increase high-frequency components in the histogram spectrum. It achieves good results by comparing the high-frequency measurement of histogram spectrum with a threshold. But it is not convenient to use in practice as there are some parameters to be determined. What is more is that some corresponding anti-forensic algorithms have been put forward. In this work, we propose a novel contrast enhancement detection approach using inter-channel similarities of high-frequency components. In comparison with the algorithm described in [1], the performance of our method is presented based on experimental results under both forensic and anti-forensic scenarios.

The remainder of this paper is organized as follows. Section 2 briefly reviews the method in [1]. Section 3 describes the proposed detection scheme in details. Experimental results and conclusions are provided in Section 4 and Section 5, respectively.

2. HISTOGRAM-BASED DETECTION OF CONTRAST ENHANCEMENT

Due to observational noise [2], sampling effects, complex lighting environments and CFA interpolation, image histograms do not contain sudden zeros or impulsive peaks. So the variation of the histogram of an unaltered image is low, while contrast enhancement manipulation will expand or squeeze the original histogram and lead to sudden peaks and gaps in the histogram, which causes the increase of high-frequency energy in the histogram spectrum. Based on this observation, Stamm and Liu proposed a general contrast enhancement detection algorithm [1] as follows.

(1) Obtain the image's histogram $h(x)$ and calculate the modified histogram $g(x)$ as follows,

$$g(x) = h(x)p(x) \tag{1}$$

where $p(x)$ is a pinch off function, whose role is to eliminate the low end or high end saturated effect in images.

(2) Transform $g(x)$ into the discrete Fourier frequency domain, $G(k)$, and calculate the high-frequency measurement F according to

$$F = \frac{1}{N}\sum_{k} \left|\beta(k)G(k)\right|, k = 0, 1, ..., 255 \tag{2}$$

where N is the total number of pixels, and $\beta(k)$ is the cutoff function deemphasizing the low frequency components of $G(k)$:

$$\beta(k) = \begin{cases} 1, T \leq k \leq 255 - T \\ 0, \text{else} \end{cases} \tag{3}$$

where T corresponds to a desired cutoff frequency.

(3) Finally, F is compared with a threshold τ to determine whether contrast enhancement has been applied.

Local contrast enhancement can be detected through applying the above procedures block by block. But there are some parameters need to be determined by users, such as the pinch off function and the cutoff frequency T. It is not convenient in practice as the optimal parameters may vary with different forms of contrast enhancements. Most importantly, as the histogram of image can be easily tampered, this kind of histogram-based forensic methods will fail if the traces left on the image histogram have been concealed by attackers. For example, Cao et al. remove the peak and gap artifacts of histogram introduced by contrast enhancement using local random dithering [3], which essentially adds Gaussian noise with appropriate variance onto the contrast enhanced image. In [4], Barni et al. also propose a universal anti-forensic technique against histogram-based contrast enhancement detector. The histogram h_y of an enhanced image is modified according to the most similar histogram h_x from a reference histogram database while keeping the image distortion as low as possible.

3. PROPOSED ALGORITHM

3.1. Motivation

In the imaging process of most commercial digital cameras, a color filter array (CFA) is placed before the sensor to capture one of the primary colors for each pixel while the other color components are interpolated with a specific demosaicking algorithm. Consider a color image composed of R, G and B channels. As human eyes are more sensitive to the green components of visible light, most CFAs tend to sample the G channel at a higher rate than R and B channels. Given any natural image sampled on the Bayer CFA, one of the constraints imposed by most demosaicking methods is that high frequencies between G and R, B channels are largely identical [5, 6]. This is effective and important because after sampling on the CFA, the G channel has twice the number of samples compared to R or B and is hence relatively free of aliasing. The consequence produced by the constraint can be represented as

$$R_h \approx G_h \approx B_h \tag{4}$$

where R_h, G_h and B_h denote the high-frequency bands of interpolated color plane R, G and B. Equation (4) can be interpreted as that R and B "copies" the high-frequency components of G [7]. However, this inter-channel similarity may be altered by some image manipulations, one of which is contrast enhancement. The reasons will be investigated in the following sub-section.

3.2. Proposed algorithm

In this sub-section, we will first show how the contrast enhancement can disturb the inter-channel similarities of high-frequency components, and then propose our detection scheme.

To explore what will happen to the high-frequency components of an image if it is enhanced, we draw the 3D scatter plots of the average high-frequency wavelet coefficients of 100 original images and the corresponding enhanced images in Fig. 1(a) and 1(b). The coordinates of each point denote the values of R, G, and B wavelet coefficients in the diagonal subband, taken at the same pixel location. In general, the points of the original images are compactly clustered along the vector $(1, 1, 1)$, which implies the strong correlation and approximate equality of the wavelet coefficients [8]. For the enhanced images, however, the points deviate from the line suggesting the inter-channel correlation has been reduced. Next, the reasons for why a linear or nonlinear contrast enhancement can disturb the inter-channel similarity are explained as follows.

(1) Linear contrast enhancement

Consider an 8-bit image as a signal $x(n)$, and $0 \leq x(n) \leq 255$. After applying Discrete Wavelet Transform (DWT) to $x(n)$, the wavelet coefficients at level $j+1$ can be written as [9]:

$$d^{j+1}(k) = \sum_{m=0}^{p-1} h(m) x^j(2k-m) \tag{5}$$

where $h(m)$ is the coefficients of a filter, depending on the chosen wavelet function, and p is the length of $h(m)$. $x^j(n)$ is the approximation coefficients at level j, and $x^0(n) = x(n)$. If $x^j(n)$ is multiplied by a linear scaling factor w, $x^j(n)$ can be divided into two sets:

$$\begin{cases} X_1 = \{x^j(n) | w * x^j(n) \leq 255\} \\ X_2 = \{x^j(n) | w * x^j(n) > 255\} \end{cases} \tag{6}$$

Then the wavelet coefficients become:

$$\begin{aligned} \widetilde{d}^{j+1}(k) = w \sum_{x^j \in X_1} h(m) x^j(2k-m) \\ + w \sum_{x^j \in X_2} h(m) x^j(2k-m) \end{aligned} \tag{7}$$

If $w \leq 1$, then $X_2 = \varnothing$, and $\widetilde{d}^{j+1}(k) = w * d^{j+1}(k)$, which means all coefficients are multiplied by the same factor. Therefore, the inter-channel similarity still holds if we separately enhance R, G and B channel. However, it rarely happens in the cut-and-paste forgery scenario as it will result in chromatic aberration. The most common situation is that the RGB image is converted into YUV color space, and contrast enhancement will be only applied in Y channel. In this case, the inter-channel similarity will be disturbed by the mapping from YUV back to RGB. If $w > 1$, then $X_2 \neq \varnothing$, and all data in X_2 will be truncated to 255, so the approximate equality of high-frequency components will be disturbed in this case.

(2) Nonlinear contrast enhancement

As any signal can be decomposed into cosine waves, for the sake of simplicity, we take two simple 1D signals composed of a sum of two zero-phase cosinusoids for example:

$$\begin{cases} x(n) = a\cos(\omega_1 n) + c\cos(\omega_2 n) \\ y(n) = b\cos(\omega_1 n) + c\cos(\omega_2 n) \end{cases} \tag{8}$$

where ω_1 and ω_2 represent the low-frequency and high-frequency, respectively. Therefore, $x(n)$ and $y(n)$ have the same high-frequency component but different low-frequency components. If they both undergo the same nonlinear transformation function $T(x)$, then we can rewrite $T(x)$ in terms of its Taylor series expansion:

$$\begin{aligned} T(x) &= T(x_0) + T'(x_0)(x-x_0) + \frac{T''(x_0)(x-x_0)^2}{2} \\ &+ \sum_{i=3}^{\infty} \frac{T^{(i)}(x_0)(x-x_0)^i}{i!} \end{aligned} \tag{9}$$

By only considering the first three terms of the right-hand side of Equation (9), we have a $x^2(n)$ and a $y^2(n)$ term for the nonlinear transformations of $x(n)$ and $y(n)$, respectively:

$$\begin{aligned} x^2(n) &= \frac{a^2}{2}\cos(2\omega_1 n) + \frac{c^2}{2}\cos(2\omega_2 n) \\ &+ ac\cos((\omega_1-\omega_2)n) + \frac{a^2+c^2}{2} \\ &+ ac\cos((\omega_1+\omega_2)n) \end{aligned} \tag{10}$$

$$\begin{aligned} y^2(n) &= \frac{b^2}{2}\cos(2\omega_1 n) + \frac{c^2}{2}\cos(2\omega_2 n) \\ &+ bc\cos((\omega_1-\omega_2)n) + \frac{b^2+c^2}{2} \\ &+ bc\cos((\omega_1+\omega_2)n) \end{aligned} \tag{11}$$

Notice the amplitudes of new frequencies $2\omega_1$, $2\omega_2$, $\omega_1 - \omega_2$ and $\omega_1 + \omega_2$ are correlated to the amplitudes of the original frequencies, which means the equalities of high-frequency components may be disturbed by the inequalities of low-frequency components. For example, the amplitudes of the potential high-frequency $\omega_1 + \omega_2$ for $x^2(n)$ and $y^2(n)$ are no longer the same due to the inequality of the original amplitudes of ω_1. For purposes of exposition we only

consider a simplified form of a signal. However, this analysis can be generalized to more complex signals. Actually, the increasingly complex signals will aggravate the interference between different frequency components, and finally lead to the destruction of inter-channel high-frequency components.

Based on the above analysis, we propose a metric S to measure the similarity between the high-frequency components of different color channels. If the 2D wavelet coefficients of color channel c in the diagonal subband at level j is denoted by $D_c^j(m,n)$, the measurement of inter-channel similarity of high-frequency components can be defined as:

$$S = \frac{1}{MN}\sum_{m=0}^{M-1}\sum_{n=0}^{N-1}\left|D_{c_1}^1(m,n) - D_{c_2}^1(m,n)\right| \tag{12}$$

where $c_1, c_2 \in \{R,G,B\}, c_1 \neq c_2$. M and N is the width and height of the diagonal subband. A value of S greater than the decision threshold η signifies the detection of contrast enhancement. Similar to [1], we applied block-wise detection for local contrast enhancement. Conceivably, the S of unaltered image is closer to zero than that of altered image. S extracted from linear and nonlinear contrast enhanced images are shown in Fig. 2(a)-(d), which conform to our analysis above. In Fig. 2(b) and 2(c), it is straightforward to show that aside from exceptional cases, the original and enhanced images can be distinguished clearly. In Fig. (d), taking histogram equalization as a nonlinear contrast enhancement example, all the unaltered and altered images can be classified perfectly using the proposed detection scheme.

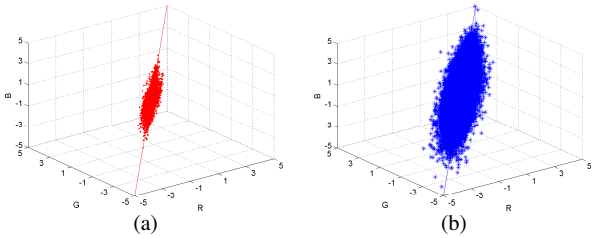

(a) (b)

Fig. 1. Scatter plots of wavelet coefficients in the diagonal subband for (a) the original images and (b) the enhanced images.

4. EXPERIMENTS

4.1. Experimental setup

To evaluate the performance of the proposed method, 100 uncompressed color images sized 1600×1200 captured by commercial cameras are used in the experiment. As in the previous work in [1, 3, 4], these images were enhanced by power law transformation (γ correction):

$$T(x) = [255(\frac{x}{255})^{\gamma}] \tag{13}$$

where $[\cdot]$ is a rounding operation, and γ is randomly chosen from the set $\{0.5;0.8;1.2;1.5;1.8;2.0\}$. These enhanced images were combined with the unaltered images to create a testing database of 700 color images. To test the performance of the proposed method on local contrast enhancement, we simply cropped blocks of different sizes from the upper-left corner of the original and γ correction enhanced images. Each block was then classified as enhanced or unaltered by our proposed detection scheme using a variety of different thresholds to get a series of receiver operating characteristic (ROC) curves. Although we gained good results for different forms

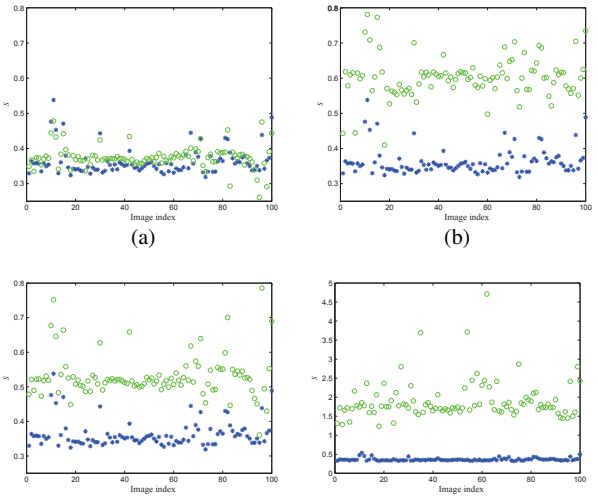

(a) (b) (c) (d)

Fig. 2. Scatter plots of S for original (blue asterisks) and enhanced (green circles) images. (a) Linear, $w = 0.6$ (R, G and B channels separated), (b) linear, $w = 0.6$, (c) linear, $w = 1.2$, (d) Histogram equalization.

of contrast enhancements such as linear enhancement and histogram equalization, the results will be shown only for γ correction. Notice that we did not enhance each color channel separately so as to avoid chromatic aberration. Instead, we converted RGB images into YUV color space and only applied contrast enhancement in Y channel as most contrast enhancement schemes do. Finally, the enhanced image will be converted back to RGB space. To provide a practical validation, we will show the detection results of a real cut-and-paste forgery.

4.2. Performance evaluation

The series of ROC curves for $c_1 = G$ and $c_2 = R$ in (12) are displayed in Fig. 3(a)-(d). P_D and P_{FA} marked in the figures denote the true positive rates and false positive rates, respectively. η is increased by 0.001 from 0 to 1.The results shown in Fig. 3 indicate that local contrast enhancement can be reliably detected even for testing blocks sized 16×16 pixels. With a P_{FA} of less than 5%, our method achieves a P_D of at least 90% using 16×16 pixels blocks for power law transformation and a P_D of around 95% using 128×128 pixels blocks. One can see that the proposed method achieves better results than Stamm's algorithm with different cutoff frequencies T in case of small blocks sized 16×16 pixels and comparable performance for large blocks sized 128×128 pixels. Because for small blocks, the statistical significance of the calculated histogram would be reduced, so it is difficult to perform reliable contrast enhancement detection for small blocks sized below 50×50 pixels using histogram-based methods like [1]. It makes sense that larger blocks are more likely to contain sufficient high-frequency evidence, but the performance of the proposed method decreases very little with the diminishing block sizes, implying the S extracted from small blocks, like 16×16 pixels, are feasible for the classification task.

An example of a cut-and-paste image forgery is shown in Fig. 4(a)-(c), where a person is cut from Fig. 4(a), then transformed using the Photoshop Curve Tools and pasted on Fig. 4(b) to produce the composite image. To detect the forgery, the image was segmented into 64×64 pixel blocks, and then our detection scheme was applied

on each block for evidence of contrast enhancement, setting $\eta = 0.67$. In Fig. 4(c), the blocks detected as contrast enhanced are highlighted in red square. Although the proposed algorithm fails on some all-white and all-black blocks as they do not contain enough high-frequency content to provide trustworthy evidence, most of the enhanced blocks are reliably detected.

4.3. Performance under anti-forensic scenario

To investigate the performance of the proposed algorithm under anti-forensic scenario, two anti-forensic schemes proposed in [3] and [4] are used.

For the method in [3], we added Gaussian noise $N(0, \sigma^2)$ to each channel of the contrast enhanced image. Detection results for image blocks sized 128×128 pixels are illustrated in Fig. 5(a)-(b). As expected, the proposed algorithm has good robustness against Gaussian noise. Because the additional noise can provide extra high-frequency evidence and therefore increase our confidence in the inter-channel similarities of high-frequency components, making it easier to detect contrast enhancement in case of additive noise.

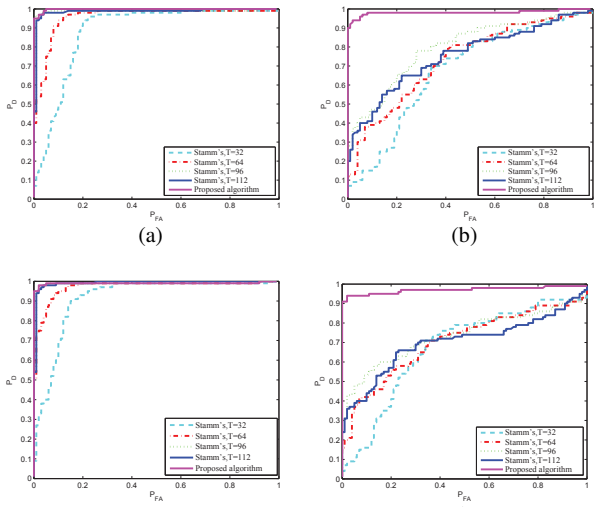

(a) (b) (c) (d)

Fig. 3. Detection ROC curves for images altered by γ correction. (a) $\gamma = 0.8$, blocksize=128×128, (b) $\gamma = 0.8$, blocksize=16×16, (c) $\gamma = 1.5$, blocksize=128×128, (d) $\gamma = 1.5$, blocksize=16×16.

(a) (b) (c)

Fig. 4. Cut-and-paste forgery detection example using 64×64 pixels blocks. (a) The original image from which an object is cut, (b) the original image onto which the cut object is pasted, (c) the detection result.

Next, for the remapping scheme described in [4], it modifies the histogram h_y of an enhanced image according to the most similar histogram h_x from a reference histogram database by pixel remapping. It is worth mentioning that instead of applying remapping in the enhanced Y channel, we remapped R, G and B channels of the enhanced image for the reason that the conversion from YUV to RGB color space is essentially a per-pixel mapping, which will again introduce artifacts into histogram and neutralize the effect of anti-forensic algorithm. The comparison between the proposed method and Stamm's in [1] is given in Fig. 5(c)-(d). As we can see, remapped images can still be detected by Stamm's algorithm when the block size is 128×128 pixels, although the histogram of anti-forensic images is smoother than that of the enhanced images. But our algorithm still obtains better result. Actually, it achieves almost perfect result since the pixel remapping scheme is highly nonlinear, which will certainly disturb the inter-channel similarity as demonstrated in Section 3.2.

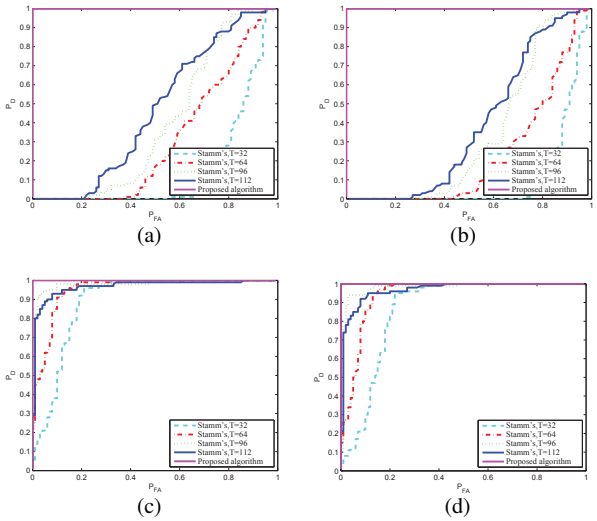

(a) (b) (c) (d)

Fig. 5. Detection ROC curves under anti-forensic scenarios. (a) $\gamma = 1.2$, $\sigma^2 = 0.01$, (b) $\gamma = 1.2$, $\sigma^2 = 0.05$, (c) $\gamma = 0.5$, blocksize=128×128, (d) $\gamma = 1.2$, blocksize=128×128.

5. CONCLUSIONS

In this paper, we present a novel forensic method to expose cut-and-paste image forgery by detecting contrast enhancement in color images. Compared with the algorithm in [1], our proposed method is easier to implement and use, good results are still gained for small blocks sized 16×16 pixels in terms of ROC curves. Besides, it has good robustness against some state-of-the-art anti-forensic schemes. When the detection block size is large enough, the traces left in the histogram can provide adequately reliable evidence, while the inter-channel similarity metric S become more convincing when block size is reduced to a certain degree. Therefore, a further enhancement would be a potential fusion of the proposed algorithm and the findings of [1]. However, both our proposed algorithm and that described in [1] suffer from poor robustness against JPEG compression, so discovering specific effects of JPEG compression on the histogram and choosing those wavelet coefficients less affected by image compression would be the main focus of our future work.

6. ACKNOWLEDGEMENT

The authors would like to express sincere gratitude to M. Barni et al. for sharing the source code of algorithm in [4].

7. REFERENCES

[1] M.C. Stamm and K.J.R. Liu, "Forensic detection of image manipulation using statistical intrinsic fingerprints," *IEEE Transactions on Information Forensics and Security*, vol. 5, no. 3, pp. 492–506, Sept. 2010.

[2] G.E. Healey and R. Kondepudy, "Radiometric ccd camera calibration and noise estimation," *IEEE Transactions on Pattern Analysis and Machine Intelligence*, vol. 16, no. 3, pp. 267–276, 1994.

[3] G. Cao, Y. Zhao, R. Ni, and H. Tian, "Anti-forensics of contrast enhancement in digital images," in *Proceedings of the 12th ACM Workshop on Multimedia and Security*, Roma, Italy, 2010, MM&Sec'10, pp. 25–34.

[4] M. Barni, M. Fontani, and B. Tondi, "A universal technique to hide traces of histogram-based image manipulations," in *Proceedings of the 14th ACM Workshop on Multimedia and Security*, Coventry, UK, 2012, MM&Sec'12, pp. 97–104.

[5] I. Pekkucuksen and Y. Altunbasak, "Edge strength filter based color filter array interpolation," *IEEE Transactions on Image Processing*, vol. 21, no. 1, pp. 393 –397, Jan. 2012.

[6] B.K. Gunturk, J. Glotzbach, Y. Altunbasak, R.W. Schafer, and R.M. Mersereau, "Demosaicking: color filter array interpolation," *IEEE Signal Processing Magazine*, vol. 22, no. 1, pp. 44–54, Jan. 2005.

[7] N.X. Lian, L. Chang, Y.P. Tan, and V. Zagorodnov, "Adaptive filtering for color filter array demosaicking," *IEEE Transactions on Image Processing*, vol. 16, no. 10, pp. 2515–2525, Oct. 2007.

[8] N.X. Lian, V. Zagorodnov, and Y.P. Tan, "Edge-preserving image denoising via optimal color space projection," *IEEE Transactions on Image Processing*, vol. 15, no. 9, pp. 2575–2587, Sept. 2006.

[9] C.L. Liu, "A tutorial of the wavelet transform," *NTUEE, Taiwan*, 2010.